CONF-780537--5

LA-UR -78-3017

TITLE: EXPANSION COOLED CO NUCLEAR PUMPED LASER

AUTHOR(S): John F. Davis
Paul F. Bird
Charles R. Mansfield
Herbert H. Helmick

SUBMITTED TO: First International Symposium on Fission Induced Plasmas and Nuclear Pumped Lasers, Orsay, France, May 23-25, 1978

los alamos
scientific laboratory
of the University of California
LOS ALAMOS, NEW MEXICO 87544

Form No. 836
St. No. 2629
1/75

UNITED STATES
ENERGY RESEARCH AND
DEVELOPMENT ADMINISTRATION
CONTRACT W-7405-ENG. 36

"EXPANSION COOLED CO NUCLEAR PUMPED LASER"*

John F. Davis, P. F. Bird
C. R. Mansfield, and H. H. Helmick
University of California
Los Alamos Scientific Laboratory
Los Alamos, New Mexico 87545

I. INTRODUCTION

A series of experiments are proposed to investigate the performance of a fission fragment excited CO laser which utilizes gas dynamic cooling. These experiments will utilize a wall source of fission fragments to provide excitation of CO or CO gas mixtures. A separate investigation will study the effects on the vibrational excitation distribution of CO or CO on gas mixtures with the addition of UF_6.

Direct discharge excited supersonically cooled CO lasers have demonstrated remarkable efficiency for converting input energy to laser output.[1-3] Continuous wave operation of carbon monoxide lasers has been achieved in which nearly 50% of the input electrical power is converted into laser output on the vibrational rotation bands.[4] This efficiency is the highest reported for any cw laser and makes the CO laser an attractive candidate for direct nuclear excitation.

Nuclear excited CO lasers have been previously studied.[5-7] As with conventional electric discharge excited CO lasers, these early nuclear excited lasers used cooling by static wall baths. The typical output power was 100 watts with an efficiency of approximately 1%. However, no attempt was made to optimize output power and efficiency.

II. EXCITATION MECHANISMS

The electronic and vibrational excitation produced in molecules by a heavy charged particle such as a fission fragment is not known in detail. The secondary

*This work supported by the Research Division, Office of Aeronautics and Space Technology, National Aeronautics and Space Administration, NASA Contract W13755 and performed under the auspices of the U.S. DOE.

electrons produced by fission fragments slowing down are responsible for the majority of the excitation in the media. These secondary electrons are expected to have a broad spectrum of initial energies, similar to the secondary electron spectra created by fast electrons. Therefore, fission fragment vibrational excitation of CO molecules in the $X'\Sigma^+$ ground state as with electron beams or electric discharges, is not expected to produce any selective excitation of any particular vibrational level, but a population distribution among the first ten or more vibrational levels that is not capable of supporting laser oscillation. Relaxation of this non-inverted population distribution then rapidly occurs by an harmonic V-V relaxation.

$$CO(v=n) + CO(v=0) \rightarrow CO(v=n-1) + CO(v=1)-\Delta E$$

This collisional process produces population inversions between the vibrational levels in a sequential way.

Other phenomena which might contribute significantly to large vibrational excitation by fission fragments occur at the end of the fission fragment path where direct transfer of momentum from the fragment to the stopping medium through close nuclear collisions will become very important. These collision processes are expected to be very efficient for production of vibrational excitation. Other important mechanisms are conversion of electronic excitation of CO molecules into vibrational excitation and excitation resulting from recombination of complexions such as $(CO)_2^+$. These reactions are shown in Table I where M indicates a third body (Ar or CO) in the reaction and the superscript (*) indicates electronic excitation.

TABLE I

$CO + FF(or\ e^-)$	$\rightarrow$	FF	$+$	$CO(v>1)$
$CO + M(recoil\ atom)$	$\rightarrow$	M	$+$	$CO(v>1)$
$CO^+ + CO\ \ (+M)$	$\rightarrow$	$(CO)_2^+\ \ (+M)$		
$(CO)_2^+ + e$	$\rightarrow$	$CO^*(+M)$	$+$	$CO(v>1)$
$CO^* + CO$	$\rightarrow$			$2 \cdot CO(v>1)$

Shown schematically in Figure 1 is an energy flow model for carbon monoxide mixed with a noble gas (in this case Argon). Not only are the processes indicated in Table I important in the gas mixture, but collisional transfer from the noble gas to the carbon monoxide may be very significant for producing vibrational excitation.

The present research is to investigate the performance of a fission fragment excited CO laser which utilizes gas dynamic cooling. From these experiments we expect to determine:

(a) Efficiency of vibrational excitation of CO by fission fragments,

(b) Distribution of excitation produced, and

(c) Vibrational excitation produced by relaxation of electronic excitation by radiation, collisions and recombination.

II. EXPERIMENTAL STUDIES

A. Apparatus

A schematic diagram of the carbon monoxide nuclear pumped gas dynamic laser is shown in Figure 2. The device basically consists of a CO high-pressure reservoir which supplies a nuclear excitation section. This section has ^{235}U foil on the walls and dimensions for optimum energy deposition at the design pressures. A nozzle then expands the excited CO to 0.01 to 0.04 atmospheres and to translation temperatures of less than 100K in the laser test section. At the end of the section a diffuser raises the gas pressure to slightly sub-atmospheric which then exhausts through a high flow rate vacuum pump.

The high pressure reservoir is a small stainless steel mix tank with four inlet 1.27 cm ID hoses from four standard high pressure cylinders and regulators with a capacity of 118000 cm^3/sec each. The nuclear section is of machined Al with removable side plates on which is mounted ^{235}U foils. A pressure measurement tap is located on the bottom wall of the nuclear section. The wall static pressure is an accurate measurement of the stagnation (no flow) pressure if the mach number (N_M) in the nuclear section is less than 0.1. The maximum calculated N_M is 0.03.

The nozzle is of rectangular cross section made of polished brass wedges with an expansion half-angle of 30^o. The true area ratio (A_{exit}/A_{throat}) is 10.1. The laser test section is also of rectangular cross-section with constant height of 5 cm and diverging side walls with an expansion half-angle of 2^o. As indicated in Figure 2, the laser test section is fitted with movable windows

for probing any region of the test section's 50 cm length. A movable pitot tube is mounted on the vertical center line of the laser test section. The small diffuser at the end of the laser test section raises the gas pressure to approximately 0.7 atmospheres. A large vacuum pump with a capacity of 1.46×10^5 cm^3/sec is attached to the diffuser and exhausts to the atmosphere.

B. Gas Dynamic Performance

For pure isentropic flow in the system, the gas parameters at any point is a function of the local mach number (N_M). Equations 1 and 2 indicate temperature and pressure relationships where the subscript 0 refers to stagnation (zero velocity) conditions and k is the ratio of specific heats.

$$\frac{To}{T} = 1 + \frac{k-1}{2} N_M^2 \qquad (1)$$

$$\frac{Po}{P} = \left(1 + \frac{k-1}{2} N_M^2\right)^{\frac{k}{k-1}} \qquad (2)$$

For isentropic flow the local mach number is determined by the area ratio of the nozzle, Equation 3, where A* is the critical area (A_{throat}) where N_M=1. Note that the N_M in the laser test section is independent of the gas temperature and pressure.

$$\frac{A}{A^*} = \frac{1}{N_M}\left[\left(\frac{2}{k+1}\right)\left(1 + \frac{k-1}{2} N_M^2\right)\right]^{\frac{k+1}{2(k-1)}} \qquad (3)$$

Due to boundary layer effects and deviations from isentropic flow, the gas parameters at any point downstream of the nozzle are a function of an effective area ratio.

By utilizing Equation 2, measuring the local pressure (p), and knowing the nuclear section pressure (p_o) one could determine the local N_M. However, surface pressure probes limit the measurements to the flow-surface interface. Using a pitot enables one to measure the axial distribution. In supersonic flow, a pitot tube does not indicate the local total pressure since a detached shock wave stands ahead of the tube. The shock is normal and the ratio of the total pressure (P_0) to measured pitot pressure (P_{02}) is related to the local mach number as shown in Equation 4 in Figure 3.

Figure 4 indicates the measured velocity profiles in the laser test section from Equation 4 using Nitrogen. It is apparent that the wedge nozzle is inadequate and a contoured nozzle should be incorporated. Between 20 and 50 cm/downstream of the nozzle throat, the velocity profile is relatively flat. For an inlet gas temperature of 295 K and a N_M of 4.16 implies a velocity of 6.89×10^4 cm/sec in the laser test section. The velocity in the nuclear section is approximately 1×10^3 cm/sec. For a stagnation pressure of 5 atmospheres, the laser test section pressure is 20.7 torr at 66.1K. The vapor pressure of CO at this temperature is 47 torr and, therefore, there is no problem with condensation.[8]

A series of measurements were also conducted where the ratio of a noble gas (Argon) and a diatomic gas (Nitrogen) was varied. Figures 5, 6, and 7 show the results of these measurements at one point in the test section. The dots are measured values and the solid line is the theoretical curve assuming an effective area ratio.

III. DISCUSSION

The nozzle and laser test section gas dynamic performance is satisfactory and laser parameters may be varied as indicated in Figures 4,5 and 6. A change in wedge nozzles would produce a new A/A* (Equation 3) and define a new N_M in the laser test section with a new series of laser parameters versus inlet gas temperatures and pressure.

Considering the nuclear section, fission events in the U^{235} walls produce excitation in the gas. Neutrons to produce these fissions are furnished by the Godiva IV pulsed reactor which can produce thermal fluxes at the laser on the order of 3.3×10^{16} n/cm^2 sec and a total fluence of 3.5×10^{12} n/cm^2 with a FWHM of 150 microseconds. The range of an average fission fragment in carbon monoxide at standard temperature and pressures is approximately 2.4 cm. At the nuclear section's operating pressure of 5 atmospheres, an average fragment will have a range of approximately 0.5 cm. The energy deposited in the gas due to a typical Godiva burst is given in Equation 5, where Φ is the thermal neutron fluence (3.5×10^{12} n/cm^2),

$$E_D = \Phi \, \Sigma_f V_f E_f \xi \qquad (5)$$

Σ_f is the macroscopic cross section (27.88 cm^{-1}), V_f is the volume of foil (1×10^{-3} cm^3/cm^2), E_f is the energy per fission (167 MeV) and ξ is the fraction of energy deposited in gas for a 5×10^{-4} cm thick foil (which is 16% efficient in emission of the fission energy).[9] The resultant energy deposited in the gas is 0.42 joules/cm^3 or 125 joules total in the nuclear test section.

In conclusion, the carbon monoxide nuclear pumped laser shows good potential of high power output with conventional means of nuclear excitation. In addition, these experiments will lead to a better understanding of fission fragment excitation of molecules and may provide insight into the potential of using molecular systems for laser power transmission.

BIBLIOGRAPHY

1. Osgood, R. M., Eppers, W. C., and Nichols, E. R., "An Investigation of the High-Power CO Laser," IEEE J. of Quantum Electronics, QE-6, 145-154, 1970.

2. Rich, J. W., Bergman, R. C., and Lordi, J. A., "Electrical Excited, Supersonic Flow Carbon Monoxide Laser," AIAA Journal, Vol. 13,95, 1975.

3. Daiber, J. W. and Thompson, H. M., "Performance of a Large, CW, Pre-excited CO Supersonic Laser," IEEE J. of Quantum Electronics, QE-13,10, 1977.

4. Bhaumik, M. L., Lacina, W. B., and Mann, M. M., "Enhancement of CO Laser Efficiency by Addition of Xenon," IEEE J. of Quantum Electronics, QE-6, 575-576, 1970.

5. McArthur, D. A. and Tollefsrud, P. B., "Observation of Laser Action in CO Gas Excited Only by Fission Fragments," Trans. Am. Nucl. Soc., 19, 356, 1974.

6. McArthur, D. A. and Tollefsrud, P. B., "Observation of Laser Action in CO Gas Excited Only with a Nuclear Reactor," Appl. Phys. Lett. 26, Feb., 1975.

7. McArthur, D. A., Schmidt, T. R., Tollefsrud, P. B., and Philibin, J. S. Trans. Amer. Nucl. Soc., 21, 1975.

8. Handbook of Chemistry and Physics, R. C. Weast, editor, 51st Edition, 1970-71, The Chemical Rubber Co., Cleveland, Ohio.

9. Gordon Hansen, Los Alamos Scientific Laboratory, private communication.

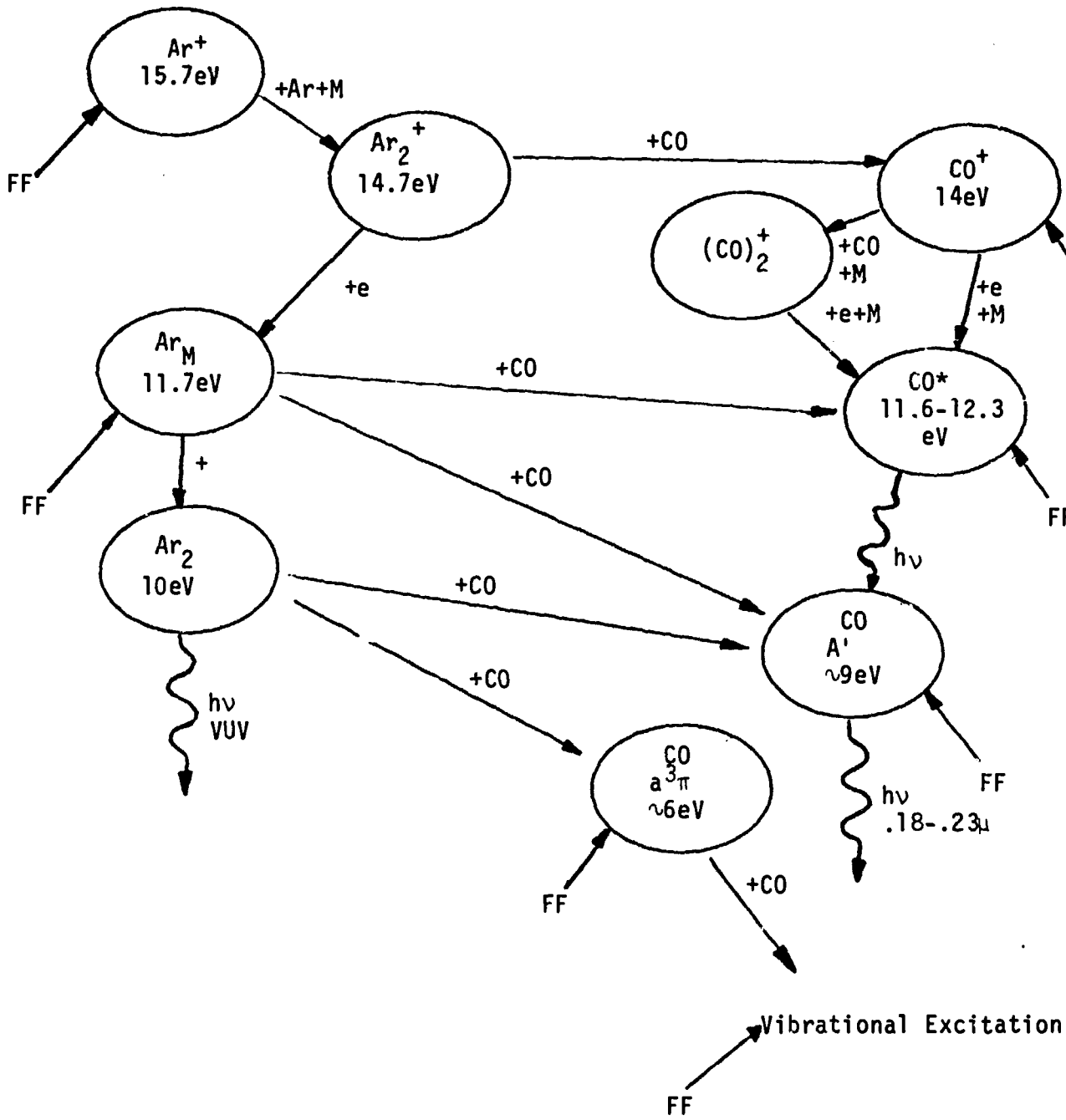

FIGURE 1. POTENTIAL ENERGY FLOW SCHEMATIC OF ARGON-CARBON MONOXIDE MIXTURES EXCITED BY FISSION FRAGMENTS

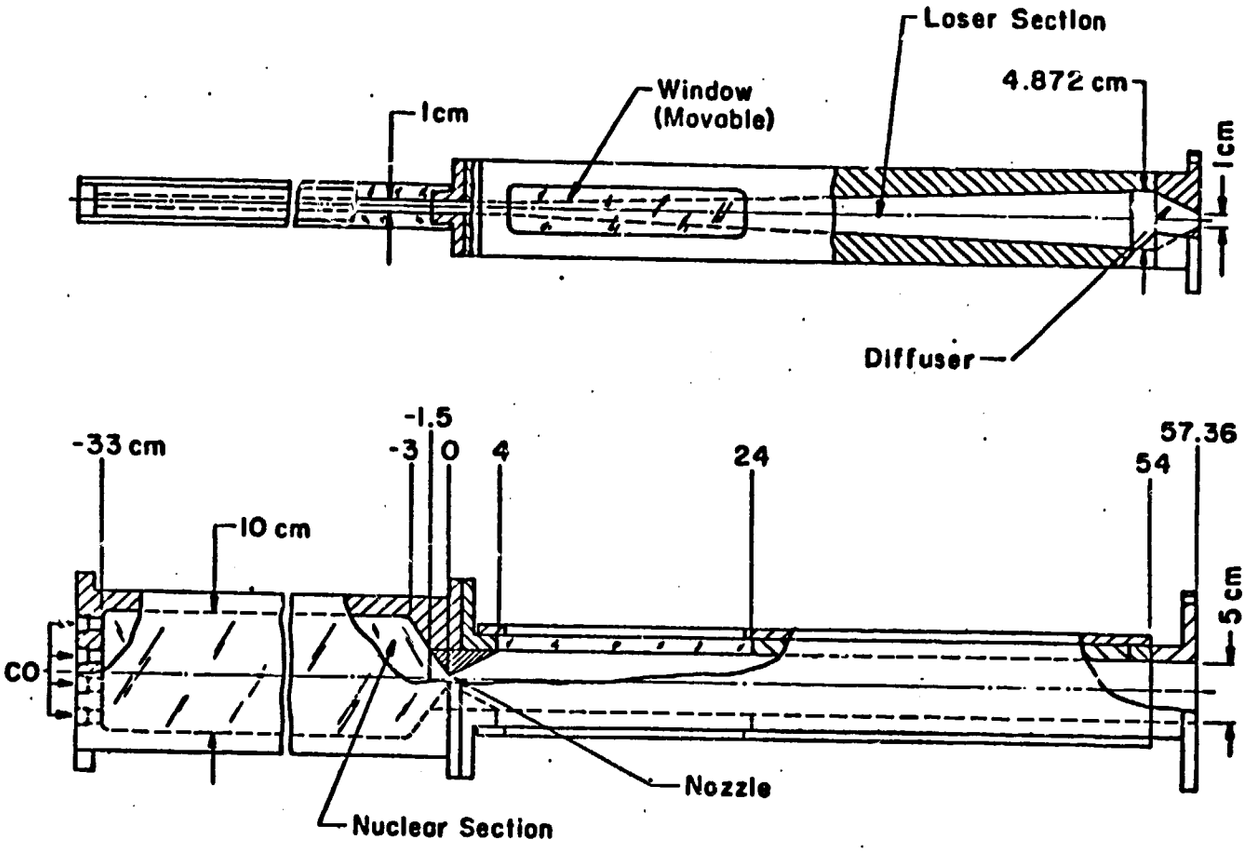

FIGURE 2. CO NPGDL

$$\frac{P_{01}}{P_{02}} = \left[\frac{2k}{k+1} N_M^2 - \frac{k-1}{k+1}\right]^{\frac{1}{k-1}} \left[\frac{1 + \frac{k-1}{2} N_M^2}{\frac{k+1}{2} N_M^2}\right]^{\frac{k}{k-1}} \qquad (4)$$

P_{01} = Reservoir Pressure (Nuclear Section)

P_{02} = Pitot Tube Pressure

k = Ratio of Specific Heats

N_M = Mach Number

FIGURE 3. PITOT TUBE FORMULA

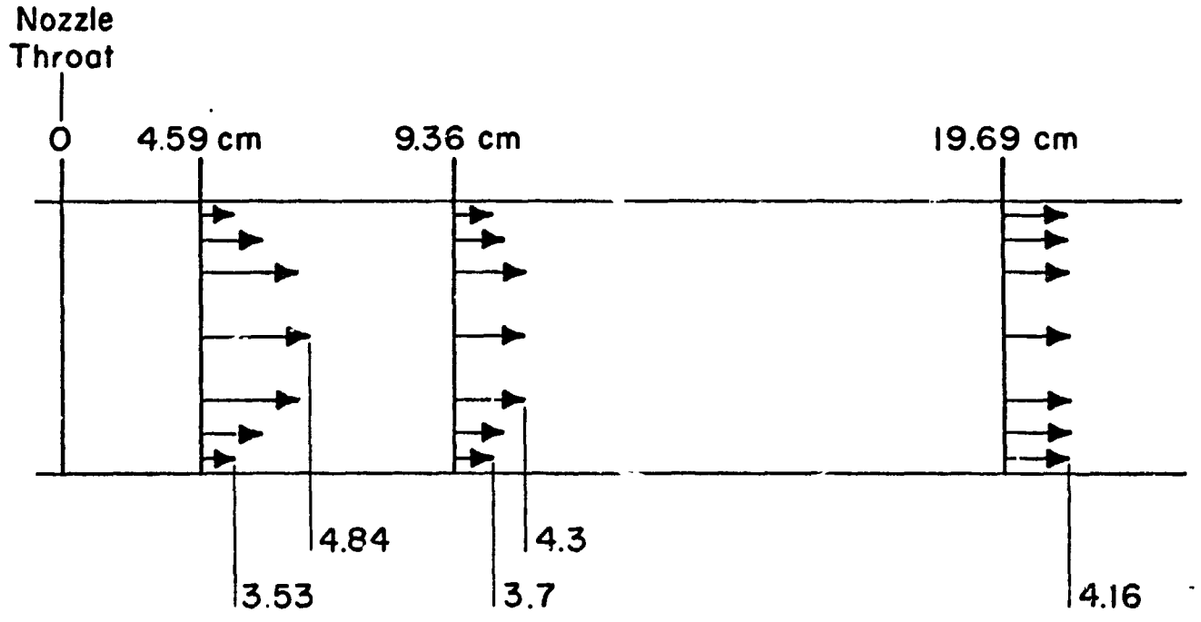

FIGURE 4. VELOCITY PROFILES (MACH NUMBER)

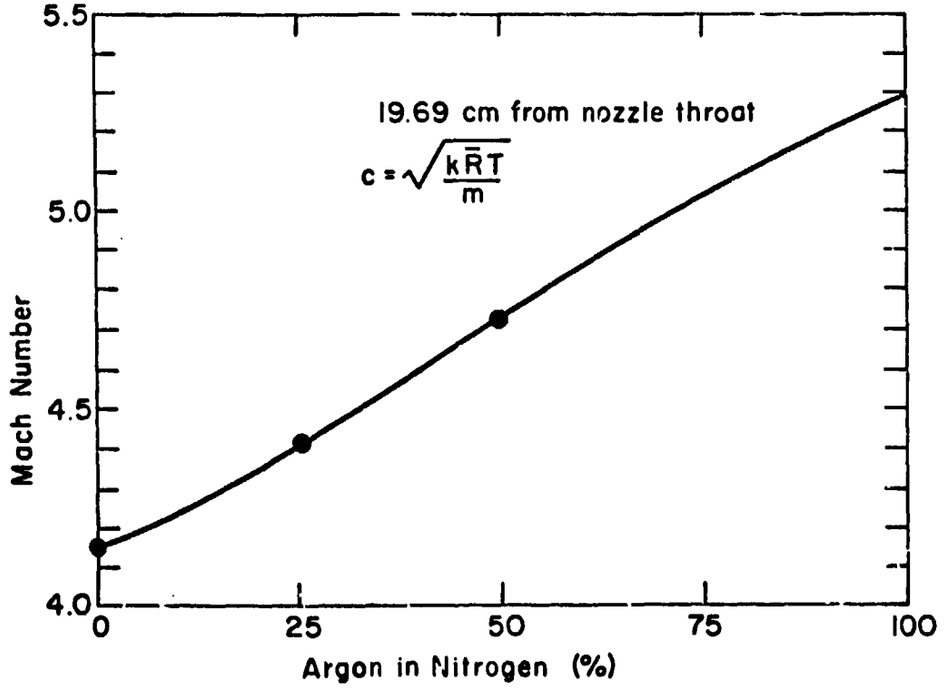

FIGURE 5. MACH NUMBER VERSUS PERCENT ARGON IN NITROGEN USING PITOT PRESSURE MEASUREMENTS 19.69 cm FROM NOZZLE THROAT AND EQUATION 4.

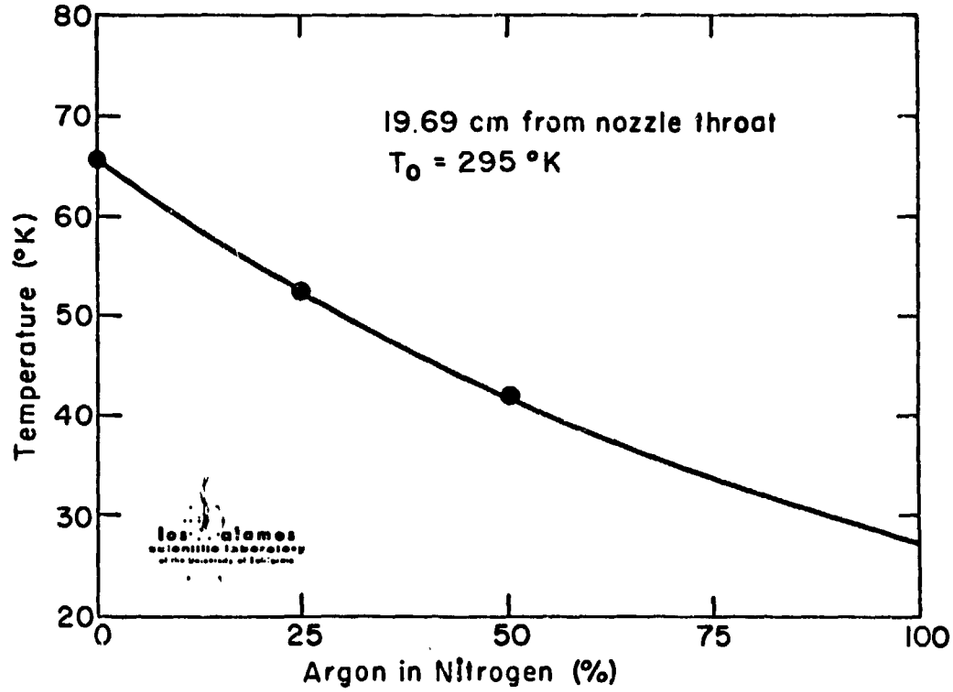

FIGURE 6. TEST SECTION TEMPERATURE VERSUS PERCENT ARGON IN NITROGEN FROM RESULTS OF FIGURE 4 AND EQUATION 1.

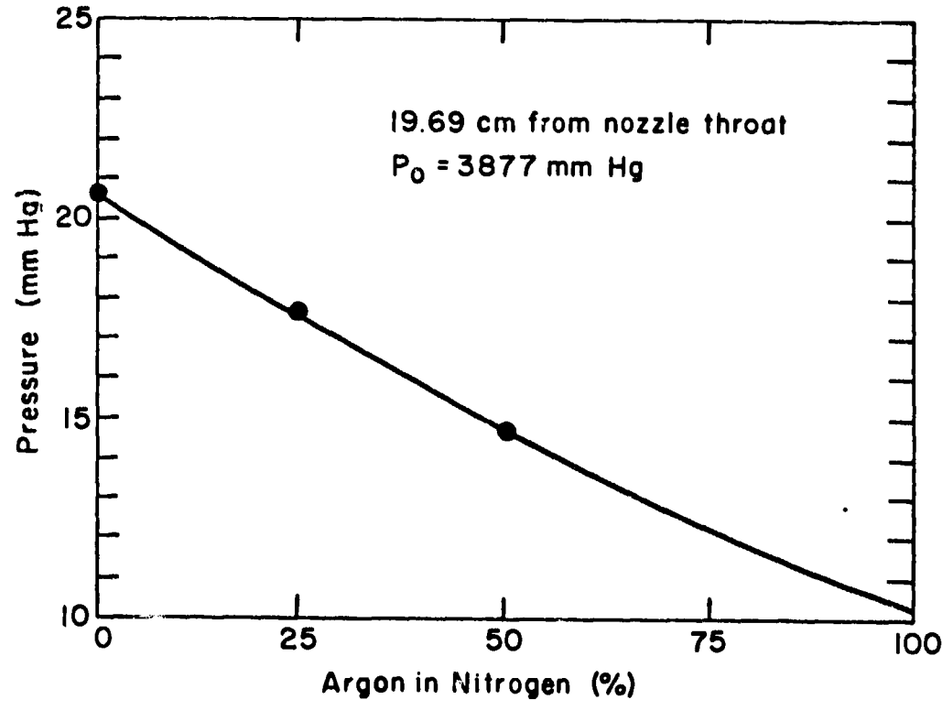

FIGURE 7. TEST SECTION PRESSURE VERSUS PERCENT ARGON IN NITROGEN FROM RESULTS OF FIGURE 4 AND EQUATION 2.